

REVIEW

Open Access



# Mantle hydration and Cl-rich fluids in the subduction forearc

Bruno Reynard<sup>1,2</sup>

## Abstract

In the forearc region, aqueous fluids are released from the subducting slab at a rate depending on its thermal state. Escaping fluids tend to rise vertically unless they meet permeability barriers such as the deformed plate interface or the Moho of the overriding plate. Channeling of fluids along the plate interface and Moho may result in fluid overpressure in the oceanic crust, precipitation of quartz from fluids, and low Poisson ratio areas associated with tremors. Above the subducting plate, the forearc mantle wedge is the place of intense reactions between dehydration fluids from the subducting slab and ultramafic rocks leading to extensive serpentinization. The plate interface is mechanically decoupled, most likely in relation to serpentinization, thereby isolating the forearc mantle wedge from convection as a cold, potentially serpentinized and buoyant, body. Geophysical studies are unique probes to the interactions between fluids and rocks in the forearc mantle, and experimental constraints on rock properties allow inferring fluid migration and fluid-rock reactions from geophysical data. Seismic velocities reveal a high degree of serpentinization of the forearc mantle in hot subduction zones, and little serpentinization in the coldest subduction zones because the warmer the subduction zone, the higher the amount of water released by dehydration of hydrothermally altered oceanic lithosphere. Interpretation of seismic data from petrophysical constrain is limited by complex effects due to anisotropy that needs to be assessed both in the analysis and interpretation of seismic data. Electrical conductivity increases with increasing fluid content and temperature of the subduction. However, the forearc mantle of Northern Cascadia, the hottest subduction zone where extensive serpentinization was first demonstrated, shows only modest electrical conductivity. Electrical conductivity may vary not only with the thermal state of the subduction zone, but also with time for a given thermal state through variations of fluid salinity. High-Cl fluids produced by serpentinization can mix with the source rocks of the volcanic arc and explain geochemical signatures of primitive magma inclusions. Signature of deep high-Cl fluids was also identified in forearc hot springs. These observations suggest the existence of fluid circulations between the forearc mantle and the hot spring hydrothermal system or the volcanic arc. Such circulations are also evidenced by recent magnetotelluric profiles.

**Keywords:** Subduction, Fluids, Forearc mantle, Salinity, Chlorine

## Review

### Introduction

The forearc region of subduction zones is a location of intense aqueous fluid circulations that influences major geologic phenomena. At shallow (~0–30 km) depth, the seismic cycle on the plate interface, with events ranging in timescale from regular earthquakes to slow earthquakes and post-seismic relaxation, is thought to depend on the

building and release of fluid pressure on fault planes fed by compaction and dehydration reactions in the subducting slab (Peacock and Wang 1999; Sleep and Blanpied 1992). Above the plate interface, such fluids interact with rocks ranging from sediments of the accretion wedge to mantle in the deepest part of the forearc region. In the shallowest part, fluids can be directly sampled at seepage, hydrothermal vent, and in mud volcanoes. They document interactions between different sources of pore water and metamorphic dehydration water from the overriding plate, subducting oceanic crust, and sediments (Kastner, et al. 2014).

Correspondence: bruno.reynard@ens-lyon.fr

<sup>1</sup>Laboratoire de Géologie de Lyon, CNRS, Ecole Normale Supérieure de Lyon, Site Monod, 15 parvis René Descartes BP7000, Lyon F-69342, France

<sup>2</sup>Université Claude Bernard Lyon 1, 43 Bd du 11 Novembre 1918, F-69622 Villeurbanne, Cedex, France

At greater depths and down to the source of magmatic liquids, connections between fluids rising to the surface and deep fluid sources are tenuous (Kawamoto, et al. 2013). Mixing of deep fluids (from more than 50 km depths) with meteoritic waters has been evidenced in hot spring. Evidence for fluid and fluid interactions with rocks may be inferred from geophysical properties such as seismic velocities and electrical conductivity, and from petrophysical modeling based on experimental data. At depths near ~20–40 km, non-volcanic tremors (Obara 2002) and other slow events occur near or above the plate interface (Dragert, et al. 2001; Rogers and Dragert 2003; Shelly, et al. 2006). These are associated with portions of the oceanic crust whose seismic properties suggest fluid overpressure (Audet, et al. 2009; Audet and Schwartz 2013). Deeper (>30 and down to 60–90 km depths), the plate interface is decoupled and seismically silent (Wada, et al. 2008), and diffuse seismicity in the oceanic crust is linked to eclogitization reactions (Hacker, et al. 2003; Kita, et al. 2006). The region above the decoupled plate interface is tectonically isolated and its nature can only be probed by geophysical means.

In the deep forearc wedge, water may be stored in the form of hydrous minerals whose presence results in seismic velocity decrease compared with anhydrous lithologies (Abers 2000; Bostock, et al. 2002; Helffrich and Abers 1997). Further decrease in seismic velocity and variations of  $V_P/V_S$  ratio is expected if excess fluid pressure develops at depths (Peacock, et al. 2011; Schubnel, et al. 2006). If fluids are connected, this will also result in variations of electrical conductivity that can be mapped by magnetotelluric surveys in subduction zones (Baba, et al. 2010; Wannamaker, et al. 2014).

Serpentine and serpentinites are candidates with which to explain the observation of reduced velocities and water storage in the forearc. Geophysical evidence for the presence of hydrated lithologies and fluids at 30–90 km depths corresponding to the deep forearc region of subduction zones will be addressed in light of recent experimental determinations of geophysical properties of serpentines and serpentinites. Interpretations of seismic velocities based on petrophysical models are simple when isotropic rock properties are considered, but become complex when different varieties of serpentine and anisotropy are taken into account. High electrical conductivities require the presence of large salinity variations in aqueous fluids in the forearc mantle. Potential links with geochemical signatures of arc magmas, hot spring fluids of deep origin, and of exhumed serpentinite bodies in high-pressure ophiolites will also be discussed.

## Geophysical observables and constrains

### *Heat flow, rheology, and geodynamical modeling*

Seismic activity, heat flow data, and geodynamical modeling (Abers, et al. 2006; Syracuse, et al. 2010; van Keken, et al. 2002; Wada and Wang 2009) are used to constrain the rheological behavior of the subduction interface. Three major segments can be distinguished. Firstly, the shallow seismogenic zone, secondly, an intermediate depth “decoupled” interface is characterized by low friction coefficient or low viscosity, and finally a deep coupled interface where the overlying mantle is entrained with the slab by viscous drag. Depths of the transitions are about 30 km between the seismogenic and decoupled zones (Hyndman and Wang 1993) and  $75 \pm 15$  km between decoupled and coupled zones as constrained from heat flow data (Wada and Wang 2009). The existence of the decoupled interface results in the formation of a static region in the forearc mantle, the so-called cold nose. This region is isolated from convection and is necessary to match the low heat flow values (Abers, et al. 2006; Wada, et al. 2008). Temperatures in the cold nose (Wada and Wang 2009) match the stability of serpentine (Ulmer and Trommsdorff 1995), the dominant hydrated phase in ultramafic compositions. The low viscosity of serpentine inferred experimentally accounts for the mechanical decoupling of the plate interface at these depths (Amiguet, et al. 2012; Chernak and Hirth 2010; Hilaret, et al. 2007; Hirauchi, et al. 2010).

### Seismology

Constrains on the structure of the forearc comes mostly from seismic tomographic studies, either arrival time tomography (Hasegawa, et al. 2008; Matsubara, et al. 2009; Nakajima, et al. 2009; Ramachandran and Hyndman 2012) or receiver function analysis (Audet, et al. 2009; Bostock, et al. 2002; Kawakatsu and Watada 2007; Nikulin, et al. 2009). Absolute velocities and velocity contrasts between different structural and lithological bodies are imaged. Another source of information is seismic anisotropy, which is sometimes derived at high resolution using both approaches above, and also with seismic wave splitting measurements (Long and van der Hilst 2006). Seismic velocities and velocity are sensitive to lithology, anisotropy, pressure, temperature, and to free fluid content especially when overpressured.

Seismological data can be compared with laboratory measurements of sound wave velocities of bulk rocks (Christensen 1996; Christensen 2004), or with petrophysical models derived from combination of single-crystal elasticity and crystal-preferred orientations in rocks (Mainprice 1990). In the absence of data on anisotropy, the isotropic approximation is justified if

rocks are isotropic, a fact that can be verified only with laboratory measurements or petrophysical calculations, or if velocities are constrained from or seismological studies with randomly oriented seismic rays. Petrophysical models and acoustic measurements along different directions give access to anisotropy. Seismic velocities obtained from petrophysical modeling (Bascou, et al. 2001; Bezacier, et al. 2010a; Bezacier, et al. 2010b; Cao, et al. 2013) are in good agreement with measurements on rock aggregates (Ji, et al. 2013; Shao, et al. 2014). They provide a basis for estimating the proportion of water stored in minerals.

Typical isotropic  $V_p/V_s$  relationships for subduction zone lithologies encountered show a nearly constant  $V_p/V_s$  ratio of 1.732 ( $\sqrt{3}$  or equivalent Poisson ratio of 0.25) for isotropic aggregates (Fig. 1a). A notable exception is quartz-rich lithologies with its lower  $V_p/V_s$  ratio of 1.6. This ratio is not, therefore, a very good indicator of lithology, and absolute values of velocities are preferable. Notable trends are those of increasing velocities in the oceanic crust accompanying transition from hydrated gabbros to dry eclogites, and a similar trend of decreasing velocities accompanying hydration (serpentinization) of peridotites. Fully serpentinized rocks have velocities similar to or lower than those of crustal rocks, which results in faint or inverted velocity contrast at the Moho (Bostock, et al. 2002). Anhydrous eclogite velocities are similar to those of dry peridotites, which results in a loss

of seismic contrast between the mantle and eclogitic oceanic crust at depths (Abers 2005).

$V_p/V_s$  relationship becomes very complex (Fig. 1b) when the large anisotropy typical of hydrated minerals and rocks is taken into account (Bezacier, et al. 2010a; Bezacier, et al. 2010b; Mainprice and Ildefonse 2009). Large seismic anisotropy of hydrated minerals is a primary cause of anisotropy in deformed rocks of subduction zones. In foliated serpentinites, the combination of intrinsic mineral anisotropy due to the layered structure of phyllosilicates and their strong alignment in deformed rocks due to the plate-shaped crystals results in a range of  $V_p/V_s$  ratio spanning most of that of typical subduction zone rocks (Bezacier, et al. 2010a). Anisotropy of blueschists is also marked because of alignment of anisotropic amphiboles and epidotes (Bezacier, et al. 2010b). Absolute velocities and  $V_p/V_s$  ratio are also drastically decreased by the presence of overpressurized fluids (Peacock, et al. 2011). Finally, in addition to modifying absolute velocities and  $V_p/V_s$  ratio, the presence of fluids or magmas damps seismic waves because of fluid motion in porosity and can be tracked by mapping seismic attenuation (Nakajima 2014).

**Magnetotellurics**

Strong constrains on fluid location is provided by electrical conductivity tomographic images (Baba, et al. 2010; Brasse and Eydam 2008; Brasse, et al. 2009; Ichiki, et al. 2009). Over the last decade, the accuracy and

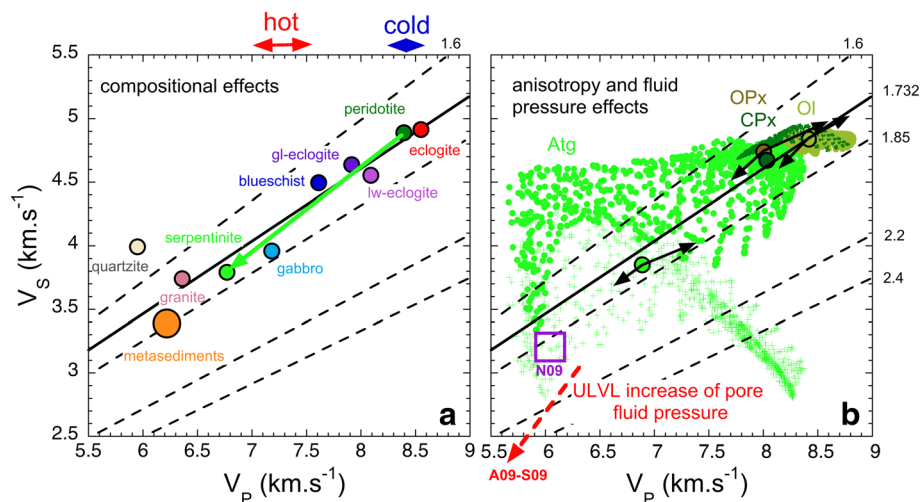
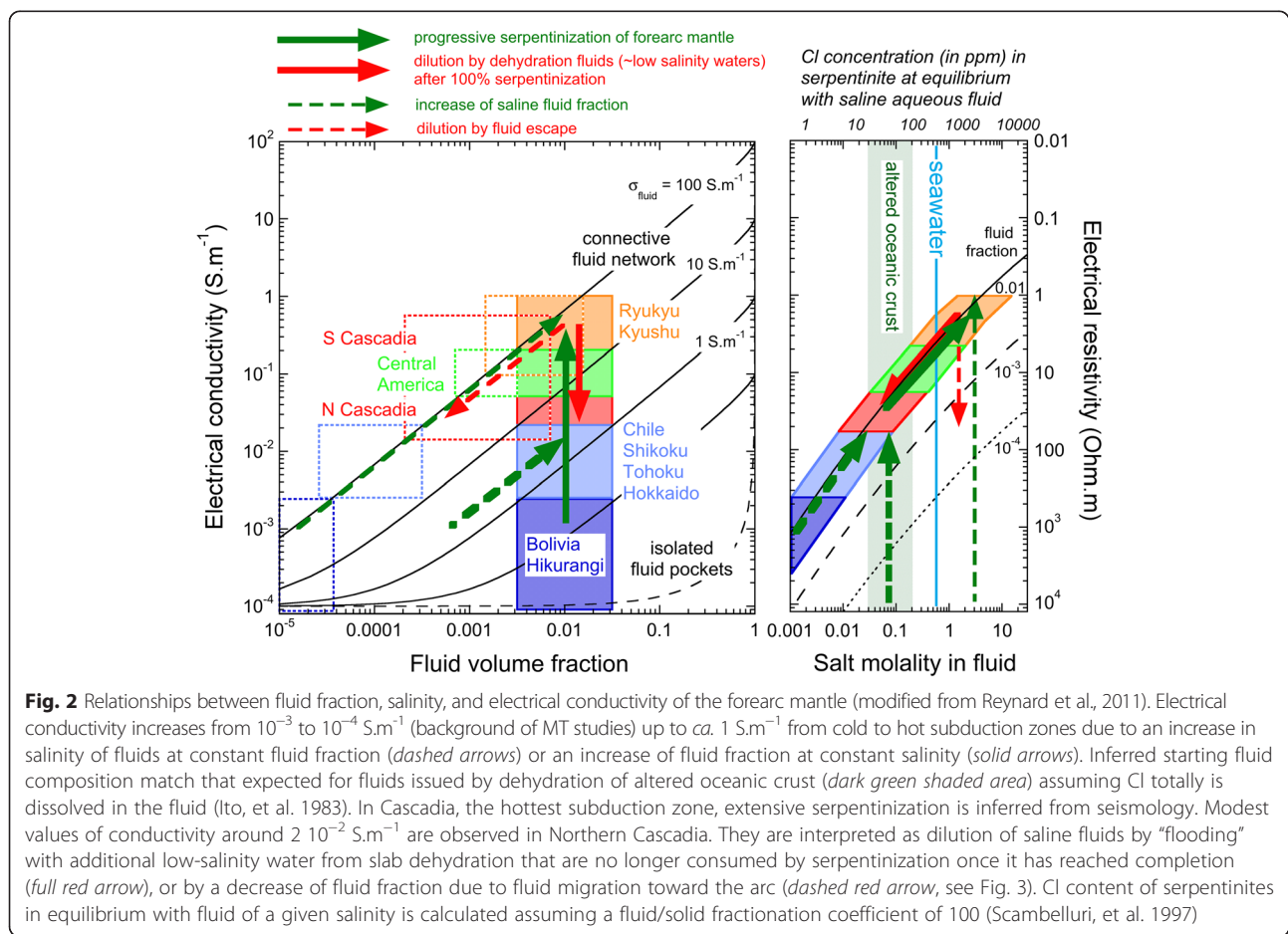


**Fig. 1** Seismic velocities of rocks and minerals representative of the various lithologies in subduction zones. **a** Isotropic sound velocities showing that most rocks except quartzite lie close to  $V_p/V_s$  ratio of  $\sqrt{3}$  or Poisson ratio of 0.25 (solid line). The effect of hydration is to reduce sound velocities (green arrow). A similar trend exists for the transformation of dry eclogite to hydrated gabbro. *Lw* and *gl* stand for lawsonite and glaucophane, respectively. **b** Effect of anisotropy in ultrabasic rocks and pore fluid overpressure (red arrow). Effects of anisotropy are especially marked in foliated serpentinites (Bezacier, et al. 2013; Bezacier, et al. 2010a) with the  $V_{s1}$  branch (full circles) and  $V_{s2}$  branch (crosses) covering a broad range of absolute velocities and  $V_p/V_s$  ratios. A foliated layer of serpentinite can explain the properties of anisotropic layers observed just above the subducting crust of Cascadia (N09, Nikulin, et al 2009). Ultra-low-velocity layers (A09-S09, Audet, et al. 2009, Song, et al. 2009) require pore fluid overpressure (Peacock, et al. 2011). *Atg* antigorite serpentinite, *CPx* clinopyroxene, *OPx* orthopyroxene, and *Ol* olivine. Olive symbols olivine aggregate and dark green symbols pyroxene-rich peridotite

resolution of 2D electrical conductivity images has greatly improved (Wannamaker, et al. 2014; Worzewski, et al. 2011) with imaging of fluid paths that can be compared with seismic tomography. Typical values of conductivity range between  $10^{-3}$  and  $10^{-4}$  and  $1 \text{ S.m}^{-1}$ , the lower values being defined by the background sensitivity in cold and fluid-poor regions, and the highest observed in zones where fluids and melts are abundant.

Laboratory measurements of electrical conductivity of earth-forming materials provide the basis for interpreting magnetotelluric data. Silicates, including both nominally anhydrous and hydrous phases such as serpentines, are poor conductors, with a small polaron-type conduction mechanism that results in high temperature dependence, and typical conductivities lower than  $10^{-3}$ – $10^{-4} \text{ S.m}^{-1}$  at temperatures of the forearc (Guo, et al. 2011; Reynard, et al. 2011). Brucite, a minor component of hydrated ultrabasic rocks, has a slightly higher conductivity, because conductivity occurs mainly by proton exchange (Fujita, et al. 2007), but is not abundant enough to explain high conductivity in hydrated ultrabasic rocks.

High conductivities of the forearc regions require the presence of an interconnected conductive fluid mixed with serpentinized peridotites because high-conductivity solids, iron oxides, sulfides, graphite, and metals are likely not sufficiently abundant to form a connective network (Kawano, et al. 2012; Reynard, et al. 2011). At the low temperatures of the forearc mantle, saline waters are the best candidates for high-conductivity fluids in the absence of melting. NaCl salt is soluble and is carried by fluid inclusions (Vanko 1988) and to a smaller extent by hydrothermal minerals (Ito, et al. 1983; Lécuyer and Reynard 1996) of the subducted lithosphere that was hydrothermally altered by seawater either at the ridge (Spooner and Fyfe 1973) or at the trench (Ranero, et al. 2003). Fluid contents and salinity are obtained by comparing model conductivities of fluid-rock mixtures with observed values in the forearc mantle (Fig. 2). The assumed (resistive) matrix and (conductive) fluid-filled pore geometry is either an assemblage of spheres or a cubic network of fractures, for which exact expressions have been derived (Waff 1974) and were used for calculations. Both



models yield virtually identical results that can be approximated by

$$\sigma_b = 2/3 F \sigma_f, \quad (1)$$

where  $\sigma_b$  is the bulk aggregate conductivity,  $F$  the fluid volume fraction, and  $\sigma_f$  the conductivity of the fluid is larger than that of the solid, with a maximum conductivity of  $10^{-4} \text{ S.m}^{-1}$  for serpentinites (Reynard, et al. 2011). Conductivities of saline fluids at high pressure and temperatures (Quist et al. 1968) allow relating fluid conductivity to salinity (Hyndman and Shearer 1989; Reynard, et al. 2011). The simple expression used by these authors has been shown to overestimate slightly conductivity at high salinities, and a more precise salinity-pressure-temperature-conductivity relationship was established from molecular dynamics (Sakuma and Ichiki 2016). Saline fluid conductivity is not very sensitive to temperature and pressure in the range of the forearc mantle (0.5–2 GPa, 573–973 K), and a simple second-order polynomial expression was fitted to experimental (Quist et al. 1968) and molecular dynamics data (Sakuma and Ichiki 2016) with a 30 % precision similar to discrepancies between datasets

$$\log \sigma_f = 1.538 + 0.7386 \log m - 0.05277 (\log m)^2, \quad (2)$$

where  $m$  is the NaCl molality in aqueous fluid.

These relations express the tradeoff between fluid fraction and salinity that cannot be independently determined for a given conductivity (Fig. 2b). The correction to saline fluid conductivities from molecular dynamics data (Sakuma and Ichiki 2016) results in a 50 % increase of maximum salinities with respect to former estimates (Hyndman and Shearer 1989; Reynard, et al. 2011), without affecting substantially their general conclusions because salinities change over more than one order of magnitude.

Highest salinities are limited by salt saturation in water, which is about 6 m for NaCl at ambient conditions, and increases with temperature and pressure. Current measurements are limited to 300 MPa over a narrow temperature range, and were fitted to a polynomial expression (Sawamura, et al. 2007). Extrapolation of this empirical fit is uncertain, but minimum values of 8–12 m are obtained at 300 MPa and 200–700 °C, which are close to the highest values estimated for explaining observed electrical conductivities (Fig. 2). These values are also above measurements of salinity in fluid inclusions from high-pressure ophiolitic rocks (Philippot, et al. 1998; Scambelluri, et al. 1997), indicating that aqueous fluids are likely undersaturated in salt at forearc conditions. The upper bound for fluid fraction is estimated as 3 %, above which the mixture is not dynamically sustainable and would collapse causing

fluid escape and release (Richard, et al. 2007). A lower bound of 0.3 % was used in the microscopic model (Fig. 2) because lower fluid fractions would be unlikely to form a connective network (Reynard, et al. 2011). However, at the resolution of magnetotelluric studies of a few kilometers or more, the existence of discrete high-porosity fault network zones separated by large impermeable blocks make lower average fractions of connective fluid realistic.

## Discussion

### Rock hydration and pore fluids from seismic observations

Simple estimations of the water stored in solids can be attempted if it is assumed that rocks are isotropic in the forearc wedge (Fig. 1a). This is reasonable in first approximation in the forearc mantle that is likely static and cold because of mechanical decoupling near the megathrust (Wada, et al. 2008). At first order, hydration is identified with serpentinitization because serpentine is the major stable hydrous mineral under the P-T conditions of the forearc wedge (Ulmer and Trommsdorff 1995). This is also a place where seismic rays used to construct tomographic images are evenly oriented and sample all velocities, a case that is not verified deeper in the slab where anisotropic effects have to be taken into account in petrophysical interpretation of seismic velocities (Reynard, et al. 2010). Seismic velocities indicate forearc mantle serpentinitization ranging from less than 10 % to up to nearly 100 % in cold and hot subduction zones, respectively (Hyndman and Peacock 2003; Reynard 2013), resulting in the latter case in the inversion of the velocity contrast at the Moho of the overriding plate (Bostock, et al. 2002). Large-scale hydration of the forearc mantle wedge by water-rich fluids released from the subducting oceanic crust was inferred from kinematic thermal modeling (Peacock 1993; Peacock and Wang 1999), and from experimental studies of dehydration reactions in slabs (Schmidt and Poli 1998). Recent coupled geodynamical-petrological modeling confirms that slab dehydration, hence potential for forearc mantle hydration, is low in cold subduction such as NE-Japan and high in hot subduction such as Cascadia of Shikoku (van Keken, et al. 2011).

Hydration of the forearc mantle wedge is caused by dehydration (or eclogitization) of the oceanic crust. Eclogitization results in the disappearance of the seismic signature of the oceanic crust at depths ranging from about 60 km in hot subduction zones down to about 150–200 km in the coldest subduction zones (Abers 2000; Helffrich and Abers 1997) where hydrated silicate lawsonite with low seismic velocities may be preserved (Chantel, et al. 2012; Reynard and Bass 2014; Schmidt and Poli 1998). Extensive dehydration of the oceanic crust is also associated with seismicity along the main Wadati-Benioff zone (Kita, et al. 2006).

Interpretation of seismic velocities is more complicated if anisotropy is taken into account (Fig. 1b). Several seismological and geological observations require taking into account seismic anisotropy or pore fluid pressure effects. In the mantle wedge near the slab, the presence of deformed serpentinites with foliation parallel to the interface is expected and can contribute to anisotropy (Katayama, et al. 2009). Anisotropic 2–5 km thick low-velocity layers at the top of the slab interface (Nikulin, et al. 2009; Park, et al. 2004) have been interpreted as deformed serpentinites (Bezacier, et al. 2013; Bezacier, et al. 2010a), but they lie at the lowest end of velocity trends in foliated serpentinites (Fig. 1b). Ultra-low-velocity layers have been observed in Cascadia and Mexico, with velocities even lower than that of the lowest ones in foliated serpentine aggregates, and  $V_P/V_S$  ratio up to 2.4 (Audet, et al. 2009; Song, et al. 2009). Ultra-low-velocity layers indicate the presence of overpressured fluids (Audet, et al. 2009; Peacock, et al. 2011; Song, et al. 2009) in what has been identified thus far with the oceanic crust, or at least its upper part. It is possible that a deformed serpentinite or sediment layer saturated with fluid contributes to the ultra-low-velocity layers near the plate interface, but this assumption is difficult to test within the resolution of seismic data. The possible combination of seismic anisotropy of the solid aggregate and of overpressured fluids in cracks (Schubnel, et al. 2006; Song and Kim 2012) makes quantitative estimation of the fluid proportion difficult.

In the serpentinitized forearc mantle wedges of hot subduction zones such as Cascadia or Shikoku (Bostock, et al. 2002; Matsubara, et al. 2009; Nakajima, et al. 2009),  $V_P/V_S$  ratios are slightly higher than those expected for isotropic serpentinite, up to 1.85 instead of 1.76 (Bezacier, et al. 2013; Bezacier, et al. 2010a). This may indicate that they are saturated with minor fluid component or have a slight anisotropy. Saturation of serpentinitized forearc mantle with fluids is consistent with high conductivities as discussed below, and with high attenuation of seismic waves (Nakajima 2014; Saita, et al. 2015).

#### Fluid composition from magnetotelluric data

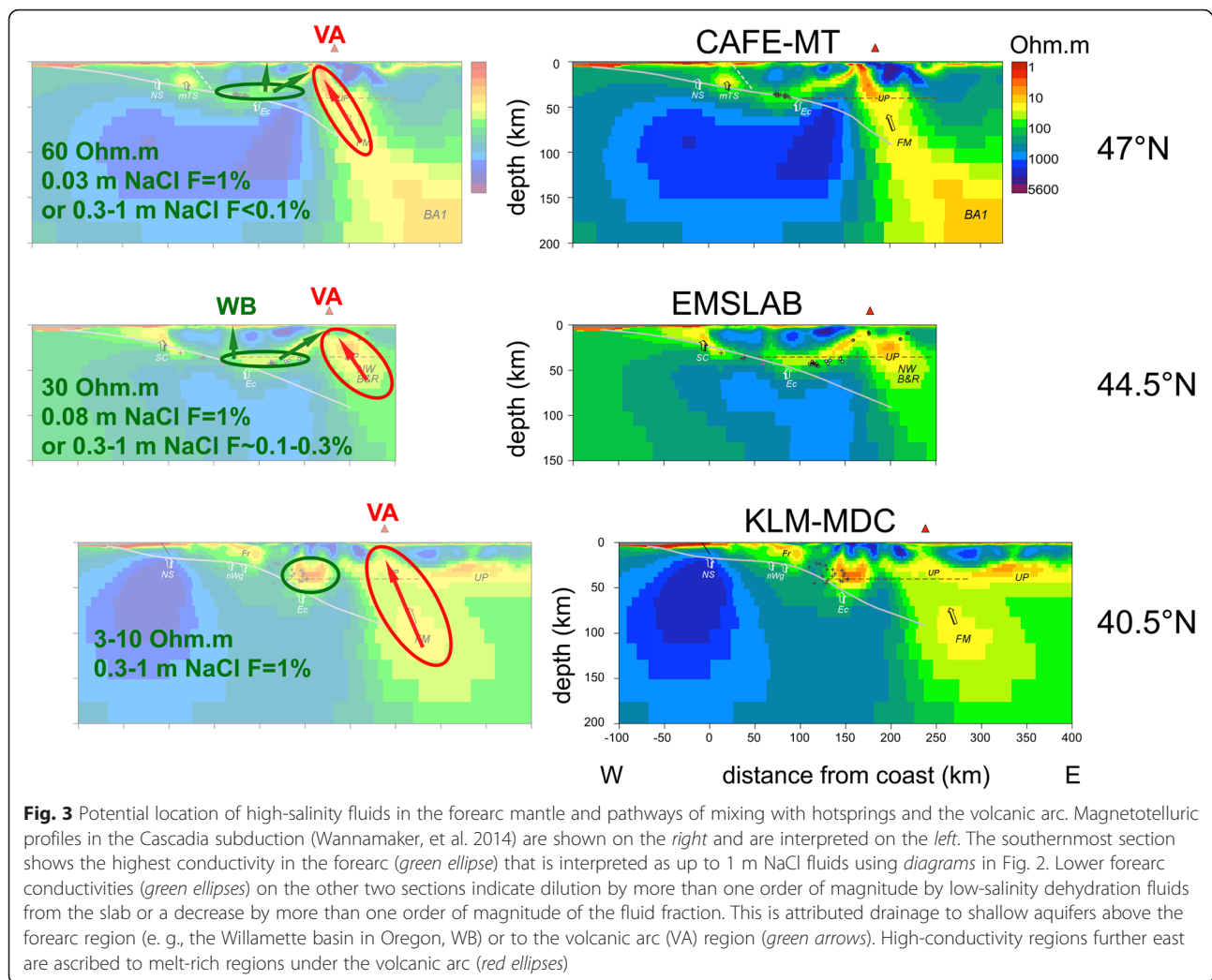
Magnetotellurics made great improvements in providing more accurate pictures of subduction zones from early studies that depicted rough limits between compartments of a few tens of kilometers to recent studies that give resolution of a few kilometers (Wannamaker, et al. 2014; Worzewski, et al. 2011). In the forearc region, the most prominent structures are high-conductivity zones that are located near the limit between the serpentinitized mantle and the base of the overriding plate (Fig. 3). Such high-conductivity zones are typical of

hot subduction zones and are absent in the cold subduction of the Pacific plate beneath Northern Honshu and Hokkaido in Japan. As argued above, high conductivities in the forearc are interpreted as saline fluids whose fraction and salinity can be estimated from conductivity (Fig. 2).

The range of conductivities observed in several subduction forearc regions shows that cold subduction displays low conductivities typical of low-fluid fractions or salinity, whereas conductivities in hot subduction zones can reach  $1 \text{ S.m}^{-1}$  which require high fluid fractions or salinity. Because of the tradeoff between fluid fraction and salinity, two extreme models can explain the observed range of conductivity, one where salinity increases from a few millimeters to a few meters at constant fluid fraction around 1 % (full arrows and filled colored fields, Fig. 2), and one where fluid fraction changes from  $10^{-5}$  to 1 % at constant high salinity (dashed arrows and dotted fields, Fig. 2).

Consumption of slightly saline fluids from the oceanic crust by serpentinitization of the forearc mantle can increase the salinity (or conductivity) of the residual fluid by a factor of up to 30 (Reynard, et al. 2011) at constant fluid fraction (thick green arrows, Fig. 2). Starting salinity of 0.05–0.1 m corresponding a mixture of subducted pore seawater with 6–12 volumes of pure water from dehydration reactions is needed (Reynard, et al. 2011). This estimate is compatible with dehydration of altered oceanic crust yielding fluids with salinity of  $\sim 0.03$ –0.2 m, or of altered oceanic crust and sediments yielding fluids with salinity of  $\sim 0.06$ –0.4 m according to their compositional range (Ito, et al. 1983). Sulfates may also contribute to salinity (Debret, et al. 2014). Salinity increases as the fluids rise and are consumed, reaching its maximum value at the top of the serpentinitized forearc mantle, where high conductivity areas are detected by magnetotelluric studies (Wannamaker, et al. 2014; Worzewski, et al. 2011). This hypothesis is supported by the fact that high conductivity are observed in hot subduction zones where serpentinitization is also detected from seismology, and not in cold subduction zones where seismic velocities suggest sluggish serpentinitization. Increase of salinity due to progressive serpentinitization was also reported in high-pressure serpentinites from the Alps (Scambelluri, et al. 1997).

With these assumptions, conductivity should increase in the forearc as the thermal parameter of the subduction zone increases. This is roughly verified since the forearc region of cold Pacific subduction beneath NE-Japan shows low conductivities when compared with hotter subduction zones (Fig. 2). There are, however, notable exceptions to this general trend. For instance, Northern Cascadia, the hottest subduction zone, shows intermediate conductivity, not the highest.



This contradiction may be resolved by considering that, as seismic data suggest (Bostock et al., 2002), the Northern Cascadia forearc mantle is already fully serpentinized and “flooded” by low-salinity water from the dehydrating slab. Because serpentinization can no longer consume pure water, the dehydration fluids will dilute the originally enriched residual waters (thick red arrow, Fig. 2). Another possibility is that saline fluids are episodically released from the high-conductivity region, thereby reducing the fluid fraction and the overall conductivity (dashed red arrow, Fig. 2). This release could feed high-salinity fluids to hot spring systems in the forearc region (Hurwitz, et al. 2005; Kusuda, et al. 2014; Masuda, et al. 1985; Nakamura, et al. 2014), or with the volcanic arc (Reynard, et al. 2011). This latter hypothesis can be discussed in light of the most recent magnetotelluric profiles, and of geochemical evidences from magmatic inclusions in arc volcanic rocks (Wallace 2005).

## Conclusions

### Geometry of fluid circulation and links with hot springs and the volcanic arc

Aqueous fluids are produced from the top of subducting plate (sedimentary cover, oceanic crust, hydrated mantle) by compaction of fractures and porosity, and by thermally induced dehydration reactions of minerals (Iwamori 1998; Peacock 1993; van Keken, et al. 2011). Vertical rise of the low-density fluids can be slowed down, impeded, or diverted by permeability barriers. Sediments like clay are well known for providing such barriers, and at depth, phyllosilicates of the clay, mica, and serpentine groups are abundant candidates for providing similar barriers. During ascent, aqueous fluids are also partly used for forming hydrated minerals (Peacock 1993).

Ultra-low-velocity layers are interpreted as overpressured fluids in portions of the oceanic crust at depths near the seismic to aseismic transition on the subduction megathrust (Audet, et al. 2009; Song, et al. 2009).

The presence of foliated phyllosilicate layers with low permeability could seal the interface between the slab and the overriding plate and account for this observation. It has been shown that foliated serpentine has anisotropic permeability that could focus fluid flow parallel to the slab up to the tip of the forearc mantle wedge (Kawano, et al. 2011). The plate interface could also be sealed by precipitation of solutes such as silica, and episodically opened by large seismic events, as suggested for Cascadia (Hyndman, et al. 2015) and other subduction zones (Audet and Burgmann 2014). The presence of fluids in the subducting oceanic crust is also suggested by high-conductivity anomalies parallel to the slab (Wannamaker, et al. 2014), and is substantiated by extensive geochemical investigations of high-pressure ophiolitic terranes (Bebout and Penniston-Dorland 2016; Deschamps, et al. 2013). Also, a consequence of salt enrichment in fluids due to hydration reactions such as serpentinization is that rocks such as serpentinites from high-pressure ophiolitic sequences should present relatively high Cl concentrations (up to several hundred or thousand ppm, Fig. 2) according to estimated water-rock partition coefficient (Scambelluri, et al. 1997).

Concentration of high-conductivity fluids at the tip of the serpentinized mantle wedge or at the base of the overriding plate is imaged in 2D electrical conductivity profiles of various subduction zones (Wannamaker, et al. 2014; Worzewski, et al. 2011). Anomalies in the Cascadia subduction profiles (Wannamaker, et al. 2014) are tentatively interpreted in terms of salinity and fluid fraction (Fig. 3), bearing in mind the tradeoff between these quantities discussed above. The highest conductivities requires fluids with salinities of the order of or above that of seawater, which can be provided by fluid release from the slab and salt enrichment by serpentinization or other partial hydration reactions (Reynard, et al. 2011). Current reports show a large range of Cl concentration in serpentinites from subduction context, suggesting interactions with high-salinity fluids at various levels (Deschamps, et al. 2013; Deschamps, et al. 2010; Lafay, et al. 2013; Scambelluri, et al. 2004; Scambelluri, et al. 1997). Cl concentrations in serpentinites that equilibrated with up to 12 m NaCl fluids should vary in the range 20–5000 ppm (Fig. 2) assuming a partition coefficient of 100 between fluids and rocks (Scambelluri, et al. 1997). Serpentinites interacting with large amounts of dehydration fluids close to the subduction interface should have low Cl content (20–100 ppm) while those of the forearc mantle should have a range of concentrations up to several thousand ppm. Obtaining Cl concentrations in serpentinites from in situ forearc context (Savov, et al. 2005) or from exhumed forearc (Deschamps, et al. 2010) could help resolve this issue.

Geochemical evidence for saline fluids of deep origins is found in hot springs of the forearc region of subduction

zones (Hurwitz, et al. 2005; Kusuda, et al. 2014; Masuda, et al. 1985; Nakamura, et al. 2014). He isotopic compositions of hydrothermal waters from the Arima district in Japan suggest interactions with the forearc mantle (Kusuda, et al. 2014), which I tentatively ascribe to serpentinization reactions, although this interpretation is not favored by the authors of the study. Whatever the case, brines mixed with meteoritic waters in hot springs are the most direct evidence of deep saline aquifers in the forearc region above the serpentinized mantle and the region where tremors are observed. Possible fluid paths between deep conductive fluids at the top the forearc or at the base of the overriding plate and shallower aquifers are highlighted as green arrows (Fig. 3) in the magnetotelluric profiles of Cascadia (Wannamaker, et al. 2014). Such paths can explain the saline brine signature in waters of the Willamette basin above the forearc of the EMSLAB profile in Oregon (Hurwitz, et al. 2005), and over whole Cascadia ranges (Mariner, et al. 1990). The observation of hot springs with salinities of about 0.1 m suggests that fluids of high salinity (0.3–1 m, Fig. 3) mixed with 3–10 volumes of dilute meteoritic waters.

Connections between deep saline fluid reservoirs at the top of the serpentinized mantle or at the base of the overriding plate and the volcanic arc are also suggested by the magnetotelluric CAFE-MT and EMSLAB profiles of Cascadia (Wannamaker, et al. 2014). Sharp high-conductivity anomalies suggest saline brines rise from the conductive anomalies of the mantle wedge to the arc through the crust following a structure dipping westward at about 30° (Fig. 3). These structures may correspond to a major fracture or fault zone, and fluid discharge to the arc could account for the lower conductive anomalies in these profiles than in the southernmost KLM-MDC profile where no such structure is observed (Wannamaker, et al. 2014). This observation supports the hypothesis of mixing of magmas with deep saline waters (Reynard, et al. 2011) to explain the high Cl/H<sub>2</sub>O ratios in magmatic inclusions of volcanic rocks from arc magmas. High Cl/H<sub>2</sub>O ratios of magmatic inclusion require the addition of Cl-rich fluids from the serpentinized wedge (Straub and Layne 2003). Fluids with salinities in the range 0.2–12 m from the cold mantle wedge (Fig. 2) account for the range of Cl/H<sub>2</sub>O ratios in magmatic inclusions up to 30 wt% equivalent NaCl, and shallow separation of saline brines due to immiscibility is required to explain the highest salt concentrations near 50 wt% (Wallace 2005).

#### Competing interests

The author declares that he has no competing interests.

#### Acknowledgements

The author is grateful to the JpGU for invitation to publish this review, to the LABEX Lyon Institute of Origins (ANR-10-LABX-0066) of the Université de Lyon for its financial support within the program "Investissements d'Avenir"

(ANR-11-IDEX-0007) of the French government operated by the National Research Agency (ANR). This work was also supported by "Programme National de Planétologie" of the "Institut National des Sciences de l'Univers", CNRS. Careful comments by two anonymous reviewers and BO Mysin helped in improving the manuscript. PE Wannamaker kindly provided the magnetotelluric profiles used in Fig. 3.

Received: 14 December 2015 Accepted: 19 April 2016

Published online: 28 April 2016

## References

- Abers GA (2000) Hydrated subducted crust at 100–250 km depth. *Earth Planet Sci Lett* 176:323–330
- Abers GA (2005) Seismic low-velocity layer at the top of subducting slabs: observations, predictions, and systematics. *Phys Earth Planet Int* 149:7–29
- Abers GA, van Keken PE, Kneller EA, Ferris A, Stachnik JC (2006) The thermal structure of subduction zones constrained by seismic imaging: implications for slab dehydration and wedge flow. *Earth Planet Sci Lett* 241:387–397
- Amiguet E, Reynard B, Caracas R, Van de Moortèle B, Hilaiert N, Wang Y (2012) Creep of phyllosilicates at the onset of plate tectonics. *Earth Planet Sci Lett* 345–348:142–150. doi:10.1016/j.epsl.2012.06.033
- Audet P, Burgmann R (2014) Possible control of subduction zone slow-earthquake periodicity by silica enrichment. *Nature* 510:389–392. doi:10.1038/nature13391
- Audet P, Schwartz S (2013) Hydrologic control of forearc strength and seismicity in the Costa Rican subduction zone. *Nat Geosci* 6:852–855. doi:10.1038/ngeo1927
- Audet P, Bostock MG, Christensen NI, Peacock SM (2009) Seismic evidence for overpressured subducted oceanic crust and megathrust fault sealing. *Nature* 457:76–78. doi:10.1038/nature07650
- Baba K, Utada H, Goto T, Kasaya T, Shimizu H, Tada N (2010) Electrical conductivity imaging of the Philippine Sea upper mantle using seafloor magnetotelluric data. *Phys Earth Planet Int* 183:44–62. doi:10.1016/j.pepi.2010.09.010
- Bascou J, Barruol G, Vauchez A, Mainprice D, Eglydio-Silva M (2001) EBSD-measured lattice-preferred orientations and seismic properties of eclogites. *Tectonophysics* 342:61–80
- Bebout GE, Penniston-Dorland SC (2016) Fluid and mass transfer at subduction interfaces—The field metamorphic record. *Lithos* 240–243:228–258. doi:10.1016/j.lithos.2015.10.007
- Bezacier L, Reynard B, Bass JD, Sanchez-Valle C, Van de Moortele BV (2010a) Elasticity of antigorite, seismic detection of serpentinites, and anisotropy in subduction zones. *Earth Planet Sci Lett* 289:198–208. doi:10.1016/j.epsl.2009.11.009
- Bezacier L, Reynard B, Bass JD, Wang J, Mainprice D (2010b) Elasticity of glaucophane, seismic velocities and anisotropy of the subducted oceanic crust. *Tectonophysics* 494:201–210. doi:10.1016/j.tecto.2010.09.011
- Bezacier L, Reynard B, Bass JD, Cardon H, Montagnac G (2013) High-pressure elasticity of serpentine, and seismic properties of the hydrated mantle wedge. *J Geophys Res-Solid Earth* 118:1–9. doi:10.1002/jgrb.50076
- Bostock MG, Hyndman RD, Rondenay S, Peacock SM (2002) An inverted continental Moho and serpentinization of the forearc mantle. *Nature* 417:536–538
- Brasse H, Eydam D (2008) Electrical conductivity beneath the Bolivian Orocline and its relation to subduction processes at the South American continental margin. *J Geophys Res Solid Earth* 113:B07109. doi:10.1029/2007jb005142
- Brasse H, Kapinos G, Mutschard L, Alvarado GE, Worzewski T, Jegen M (2009) Deep electrical resistivity structure of northwestern Costa Rica. *Geophys Res Lett* 36:L02310. doi:10.1029/2008gl036397
- Cao Y, Jung H, Song S (2013) Petro-fabrics and seismic properties of blueschist and eclogite in the North Qilian suture zone, NW China: implications for the low-velocity upper layer in subducting slab, trench-parallel seismic anisotropy, and eclogite detectability in the subduction zone. *J Geophys Res Solid Earth* 118:3037–3058. doi:10.1002/jgrb.50212
- Chantel L, Mookherjee M, Frost DJ (2012) The elasticity of lawsonite at high pressure and the origin of low velocity layers in subduction zones. *Earth Planet Sci Lett* 349–350:116–125
- Chernak LJ, Hirth G (2010) Deformation of antigorite serpentinite at high temperature and pressure. *Earth Planet Sci Lett* 296:23–33. doi:10.1016/j.epsl.2010.04.035
- Christensen NI (1996) Poisson's ratio and crustal seismology. *J Geophys Res* 101:3139–3156
- Christensen NI (2004) Serpentinites, peridotites, and seismology. *Int Geol Rev* 46:795–816
- Debert B, Koga KT, Nicollet C, Andreani M, Schwartz S (2014) F, Cl and S input via serpentinite in subduction zones: implications for the nature of the fluid released at depth. *Terra Nova* 26:96–101. doi:10.1111/ter.12074
- Deschamps F, Guillot S, Godard M, Chauvel C, Andreani M, Hattori K (2010) In situ characterizes of serpentinites from forearc mantle wedges: timing of serpentinization and behavior of fluid-mobile elements in subduction zones. *Chem Geol* 269:262–277. doi:10.1016/j.chemgeo.2009.10.002
- Deschamps F, Godard M, Guillot S, Hattori K (2013) Geochemistry of subduction zone serpentinites: A review. *Lithos* 178:96–127. doi:10.1016/j.lithos.2013.05.019
- Dragert H, Wang K, James TS (2001) A silent slip event on the deeper Cascadia subduction interface. *Science* 292:1525–1528. doi:10.1126/science.1060152
- Fujita K, Katsura T, Matsuzaki T, Ichiki M (2007) Electrical conductivity measurements of brucite under crustal pressure and temperature conditions. *Earth Planets Space* 59:645–648
- Guo X, Yoshino T, Katayama I (2011) Electrical conductivity anisotropy of deformed talc rocks and serpentinites at 3 GPa. *Phys Earth Planet Int* 188:69–81
- Hacker BR, Peacock SM, Abers GA, Holloway SD (2003) Subduction factory 2. Are intermediate-depth earthquakes in subducting slabs linked to metamorphic dehydration reactions? *J Geophys Res Solid Earth* 108 (B1):2030. doi:10.1029/2001JB001129
- Hasegawa A, Nakajima J, Kita S, Tsuji Y, Nii K, Okada T, Matsuzawa T, Zhao D (2008) Transportation of H<sub>2</sub>O in the NE Japan subduction zone as inferred from seismic observations. *J Geophys Res* 117:59–75
- Helffrich G, Abers GA (1997) Slab low-velocity layer in the eastern Aleutian subduction zone. *Geophys J Int* 130:640–648. doi:10.1111/j.1365-246X.1997.tb01858.x
- Hilaiert N, Reynard B, Wang YB, Daniel I, Merkel S, Nishiyama N, Petitgirard S (2007) High-pressure creep of serpentine, interseismic deformation, and initiation of subduction. *Science* 318:1910–1913
- Hirauchi K, Katayama I, Uehara S, Miyahara M, Takai Y (2010) Inhibition of subduction thrust earthquakes by low-temperature plastic flow in serpentine. *Earth Planet Sci Lett* 295:349–357. doi:10.1016/j.epsl.2010.04.007
- Hurwitz S, Mariner RH, Fehn U, Snyder GT (2005) Systematics of halogen elements and their radioisotopes in thermal springs of the Cascade Range, Central Oregon, Western USA. *Earth Planet Sci Lett* 235:700–714. doi:10.1016/j.epsl.2005.04.029
- Hyndman R, Peacock S (2003) Serpentinization of the forearc mantle. *Earth Planet Sci Lett* 212:417–432
- Hyndman RD, Shearer PM (1989) Water in the lower continental crust—modeling magnetotelluric and seismic-reflection results. *Geophys J Int* 98:343–365
- Hyndman RD, Wang K (1993) Thermal constraints on the zone of major thrust earthquake failure—the Cascadia subduction zone. *J Geophys Res* 98:2039–2060. doi:10.1029/92jb02279
- Hyndman RD, McCrory PA, Wech A, Kao H, Ague J (2015) Cascadia subducting plate fluids channelled to fore-arc mantle corner: ETS and silica deposition. *J Geophys Res Solid Earth* 120:4344–4358. doi:10.1002/2015jb011920
- Ichiki M, Baba K, Toh H, Fuji-Ta K (2009) An overview of electrical conductivity structures of the crust and upper mantle beneath the northwestern Pacific, the Japanese Islands, and continental East Asia. *Gondwana Res* 16:545–562. doi:10.1016/j.gr.2009.04.007
- Ito E, Harris DM, Anderson AT (1983) Alteration of oceanic crust and geologic cycling of chlorine and water. *Geochim Cosmochim Acta* 47:1613–1624. [http://dx.doi.org/10.1016/0016-7037\(83\)90188-6](http://dx.doi.org/10.1016/0016-7037(83)90188-6)
- Iwamori H (1998) Transportation of H<sub>2</sub>O and melting in subduction zones. *Earth Planet Sci Lett* 160:65–80. doi:10.1016/s0012-821x(98)00080-6
- Ji S, Shao T, Michibayashi K, Long C, Wang Q, Kondo Y, Zhao W, Wang H, Salisbury MH (2013) A new calibration of seismic velocities, anisotropy, fabrics, and elastic moduli of amphibole-rich rocks. *J Geophys Res Solid Earth* 118:4699–4728. doi:10.1002/jgrb.50352
- Kastner M, Solomon EA, Harris RN, Torres ME (2014) Chapter 4.4.3 - Fluid Origins, Thermal Regimes, and Fluid and Solute Fluxes in the Forearc of Subduction Zones. In: Ruediger Stein DKBF, Hans-Christian L (eds) *Developments in Marine Geology*, vol Volume 7. Amsterdam, Netherlands: Elsevier. pp 671–733. doi:10.1016/B978-0-444-62617-2.00022-0
- Katayama I, Hirauchi H, Michibayashi K, Ando J (2009) Trench-parallel anisotropy produced by serpentine deformation in the hydrated mantle wedge. *Nature* 461:1114–1118. doi:10.1038/nature08513
- Kawakatsu H, Watada S (2007) Seismic evidence for deep-water transportation in the mantle. *Science* 316:1468–1471
- Kawamoto T, Yoshikawa M, Kumagai Y, Mirabueno M, Okuno M, Kobayashi T (2013) Mantle wedge infiltrated with saline fluids from dehydration and decarbonation of subducting slab. *Proc Natl Acad Sci U S A* 110:9663–9668

- Kawano S, Katayama I, Okazaki K (2011) Permeability anisotropy of serpentinite and fluid pathways in a subduction zone. *Geology* 39:939–942. doi:10.1130/g32173.1
- Kawano S, Yoshino T, Katayama I (2012) Electrical conductivity of magnetite-bearing serpentinite during shear deformation. *Geophys Res Lett* 39. doi:10.1029/2012GL053652
- Kita S, Okada T, Nakajima J, Matsuzawa T, Hasegawa A (2006) Existence of a seismic belt in the upper plane of the double seismic zone extending in the along-arc direction at depths of 70–100 km beneath NE Japan. *Geophys Res Lett* 33:L24310. doi:10.1029/2006gl028239
- Kusuda C, Iwamori H, Nakamura H, Kazahaya K, Morikawa N (2014) Arima hot spring waters as a deep-seated brine from subducting slab. *Earth Planets Space* 66:119
- Lafay R, Deschamps F, Schwartz S, Guillot S, Godard M, Debret B, Nicollet C (2013) High-pressure serpentinites, a trap-and-release system controlled by metamorphic conditions: example from the Piedmont zone of the western Alps. *Chem Geol* 343:38–54. doi:10.1016/j.chemgeo.2013.02.008
- Lécuyer C, Reynard B (1996) High-temperature alteration of oceanic gabbros by seawater (Hess Deep, Ocean Drilling Program Leg 147): evidence from oxygen isotopes and elemental fluxes. *J Geophys Res Solid Earth* 101:15883–15897
- Long MD, van der Hilst RD (2006) Shear wave splitting from local events beneath the Ryukyu arc: trench-parallel anisotropy in the mantle wedge. *Phys Earth Planet Int* 155:300–312. doi:10.1016/j.pepi.2006.01.003
- Mainprice D (1990) An efficient FORTRAN program to calculate seismic anisotropy from the lattice preferred orientation of minerals. *Comput Geosci* 16:385–393
- Mainprice D, Ildefonse B (2009) Seismic anisotropy of subduction zone minerals—Contribution of hydrous phases. In: *Subduction zone geodynamics*, vol. Springer, Berlin Heidelberg, pp 63–84
- Mariner RH, Presser TS, Evans WC, Pringle MKW (1990) Discharge rates of fluid and heat by thermal springs of the Cascade Range, Washington, Oregon, and northern California. *J Geophys Res Solid Earth* 95:19517–19531. doi:10.1029/JB095iB12p19517
- Masuda H, Sakai H, Chiba H, Tsurumaki M (1985) Geochemical characteristics of Na-Ca-Cl-HCO<sub>3</sub> type waters in Arima and its vicinity in the western Kinki district, Japan. *Geochem J* 19:149–162
- Matsubara M, Obara K, Kasahara K (2009) High-VP/VS zone accompanying non-volcanic tremors and slow-slip events beneath southwestern Japan. *Tectonophysics* 472:6–17
- Nakajima J (2014) Seismic attenuation beneath Kanto, Japan: evidence for high attenuation in the serpentinized subducting mantle. *Earth Planets Space* 66: 12. doi:10.1186/1880-5981-66-12
- Nakajima J, Tsuji Y, Hasegawa A, Kita S, Okada T, Matsuzawa T (2009) Tomographic imaging of hydrated crust and mantle in the subducting Pacific slab beneath Hokkaido, Japan: evidence for dehydration embrittlement as a cause of intraslab earthquakes. *Gondwana Res* 16: 470–481. doi:10.1016/j.gr.2008.12.010
- Nakamura H, Fujita Y, Nakai S, Yokoyama T, Iwamori H (2014) Rare earth elements and Sr-Nd-Pb isotopic analyses of the Arima hot spring waters, Southwest Japan: implications for origin of the Arima-type brine. *J Geol Geosci* 3:161
- Nikulin A, Levin V, Park J (2009) Receiver function study of the Cascadia megathrust: Evidence for localized serpentinization. *Geochemistry, Geophysics, Geosystems* 10(7). doi:10.1029/2009GC002376
- Obara K (2002) Nonvolcanic deep tremor associated with subduction in southwest Japan. *Science* 296:1679–1681
- Park J, Yuan H, Levin V (2004) Subduction zone anisotropy beneath Corvallis, Oregon: A serpentinite skid mark of trench-parallel terrane migration? *J Geophys Res Solid Earth* 109:B10306. doi:10.1029/2003JB002718
- Peacock S (1993) Large-scale hydration of the lithosphere above subducting slabs. *Chem Geol* 108:49–59
- Peacock SM, Wang K (1999) Seismic consequences of warm versus cool subduction metamorphism: examples from southwest and northeast Japan. *Science* 286:937–939
- Peacock SM, Christensen NI, Bostock MG, Audet P (2011) High pore pressures and porosity at 35 km depth in the Cascadia subduction zone. *Geology* 39: 471–474. doi:10.1130/g31649.1
- Philippot P, Agrinier P, Scambelluri M (1998) Chlorine cycling during subduction of altered oceanic crust. *Earth Planet Sci Lett* 161:33–44, [http://dx.doi.org/10.1016/S0012-821X\(98\)00134-4](http://dx.doi.org/10.1016/S0012-821X(98)00134-4)
- Quist AS, Marshall WL (1968) Electrical conductances of aqueous sodium chloride solutions from 0 to 800 degrees and at pressures to 4000 bars. *Journal of Physical Chemistry* 72 (2):684–703.
- Ramachandran K, Hyndman RD (2012) The fate of fluids released from subducting slab in Northern Cascadia. *Solid Earth* 3:121–129. doi:10.5194/se-3-121-2012
- Ranero CR, Morgan JP, McIntosh K, Reichert C (2003) Bending-related faulting and mantle serpentinization at the Middle America trench. *Nature* 425:367–373. doi:10.1038/nature01961
- Reynard B (2013) Serpentine in active subduction zones. *Lithos* 178:171–185, <http://dx.doi.org/10.1016/j.lithos.2012.10.012>
- Reynard B, Bass JD (2014) Elasticity of lawsonite and seismological signature of metamorphism and water cycling in the subducting oceanic crust. *J Metam Geol* 32:479–487. doi:10.1111/jmg.12072
- Reynard B, Nakajima J, Kawakatsu H (2010) Earthquakes and plastic deformation of anhydrous slab mantle in double Wadati Benioff zones. *Geophys Res Lett* 37. doi:10.1029/2010GL045494
- Reynard B, Mibe K, Van de Moortele B (2011) Electrical conductivity of the serpentinized mantle and fluid flow in subduction zones. *Earth Planet Sci Lett* 307:387–394. doi:10.1016/j.epsl.2011.05.013
- Richard G, Monnerieu M, Rabinowicz M (2007) Slab dehydration and fluid migration at the base of the upper mantle: implications for deep earthquake mechanisms. *Geophys J Int* 168:1291–1304. doi:10.1111/j.1365-246X.2006.03244.x
- Rogers G, Dragert H (2003) Episodic tremor and slip on the Cascadia subduction zone: the chatter of silent slip. *Science* 300:1942–1943
- Saita H, Nakajima J, Shiina T, Kimura JI (2015) Slab-derived fluids, fore-arc hydration, and sub-arc magmatism beneath Kyushu, Japan. *Geophys Res Lett* 42:1685–1693. doi:10.1002/2015GL063084
- Sakuma H, Ichiki M (2016) Electrical conductivity of NaCl-H<sub>2</sub>O fluid in the crust. *J Geophys Res Solid Earth*. doi:10.1002/2015JB012219
- Savov IP, Ryan JG, D'Antonio M, Kelley K, Mattie P (2005) Geochemistry of serpentinized peridotites from the Mariana Forearc Conical Seamount, ODP Leg 125: implications for the elemental recycling at subduction zones. *Geochem Geophys Geosys* 6 doi:10.1029/2004gc000777
- Sawamura S, Egoshi N, Setoguchi Y, Matsuo H (2007) Solubility of sodium chloride in water under high pressure. *Fluid Phase Equilib* 254:158–162, <http://dx.doi.org/10.1016/j.fluid.2007.03.003>
- Scambelluri M, Piccardo GB, Philippot P, Robbiano A, Negretti L (1997) High salinity fluid inclusions formed from recycled seawater in deeply subducted alpine serpentinite. *Earth Planet Sci Lett* 148:485–499
- Scambelluri M, Muntener O, Ottolini L, Pettke TT, Vannucci R (2004) The fate of B, Cl and Li in the subducted oceanic mantle and in the antigorite breakdown fluids. *Earth Planet Sci Lett* 222:217–234. doi:10.1016/j.epsl.2004.02.012
- Schmidt M, Poli S (1998) Experimentally based water budgets for dehydrating slabs and consequences for arc magma generation. *Earth Planet Sci Lett* 163:361–379
- Schubnel A, Benson P, Thompson B, Hazzard J, Young RP (2006) Quantifying damage, saturation and anisotropy in cracked rocks by inverting elastic wave velocities. In: Dresen G, Zang A, Stephansson O (eds) *Rock damage and fluid transport, part I*, vol. Birkhäuser, Basel, pp 947–973
- Shao T, Ji S, Kondo Y, Michibayashi K, Wang Q, Xu Z, Sun S, Marcotte D, Salisbury MH (2014) Antigorite-induced seismic anisotropy and implications for deformation in subduction zones and the Tibetan Plateau. *J Geophys Res Solid Earth* 119:2068–2099. doi:10.1002/2013jb010661
- Shelly DR, Beroza GC, Ide S, Nakamura S (2006) Low-frequency earthquakes in Shikoku, Japan, and their relationship to episodic tremor and slip. *Nature* 442:188–191. doi:10.1038/nature04931
- Sleep NH, Blanpied ML (1992) Creep, compaction, and the weak rheology of major faults. *Nature* 359:687–692. doi:10.1038/359687a0
- Song TRA, Kim Y (2012) Localized seismic anisotropy associated with long-term slow-slip events beneath southern Mexico. *Geophys Res Lett* 39:6. doi:10.1029/2012gl051324
- Song TRA, Helmberger DV, Brudzinski MR, Clayton RW, Davis P, Perez-Campos X, Singh SK (2009) Subducting slab ultra-slow velocity layer coincident with silent earthquakes in southern Mexico. *Science* 324:502–506. doi:10.1126/science.1167595
- Spooner ETC, Fyfe WS (1973) Sub-sea-floor metamorphism, heat and mass-transfer. *Contrib Mineral Petrol* 42:287–304. doi:10.1007/bf00372607
- Straub SM, Layne GD (2003) Decoupling of fluids and fluid-mobile elements during shallow subduction: evidence from halogen-rich andesite melt inclusions from the Izu arc volcanic front. *Geochem Geophys Geosyst* 4:9003. doi:10.1029/2002gc000349
- Syracuse EM, van Keken PE, Abers GA (2010) The global range of subduction zone thermal models. *Phys Earth Planet Int* 183:73–90. doi:10.1016/j.pepi.2010.02.004
- Ulmer P, Trommsdorff V (1995) Serpentine stability to mantle depths and subduction-related magmatism. *Science* 268:858–861

- van Keken PE, Kiefer B, Peacock SM (2002) High-resolution models of subduction zones: implications for mineral dehydration reactions and the transport of water into the deep mantle. *Geochemistry Geophysics Geosystems* 3. doi:10.1029/2001gc000256
- van Keken PE, Hacker BR, Syracuse EM, Abers GA (2011) Subduction factory 4. Depth-dependent flux of H<sub>2</sub>O from subducting slabs worldwide. *J Geophys Res Solid Earth* 116. doi:10.1029/2010jb007922
- Vanko DA (1988) Temperature, pressure, and composition of hydrothermal fluids, with their bearing on the magnitude of tectonic uplift at mid-ocean ridges, inferred from fluid inclusions in oceanic layer 3 rocks. *J Geophys Res Solid Earth* 93:4595–4611. doi:10.1029/JB093iB05p04595
- Wada I, Wang KL (2009) Common depth of slab-mantle decoupling: reconciling diversity and uniformity of subduction zones. *Geochemistry Geophysics Geosystems* 10. doi:10.1029/2009gc002570
- Wada I, Wang KL, He JG, Hyndman RD (2008) Weakening of the subduction interface and its effects on surface heat flow, slab dehydration, and mantle wedge serpentinization. *J Geophys Res Solid Earth* 113(B4). doi:10.1029/2007JB005190
- Waff HS (1974) Theoretical considerations of electrical conductivity in a partially molten mantle and implications for geothermometry. *J Geophys Res* 79:4003–4010
- Wallace PJ (2005) Volatiles in subduction zone magmas: concentrations and fluxes based on melt inclusion and volcanic gas data. *J Volcanol Geotherm Res* 140:217–240. doi:10.1016/j.jvolgeores.2004.07.023
- Wannamaker PE, Evans RL, Bedrosian PA, Unsworth MJ, Maris V, McGary RS (2014) Segmentation of plate coupling, fate of subduction fluids, and modes of arc magmatism in Cascadia, inferred from magnetotelluric resistivity. *Geochem Geophys Geosys* 15:4230–4253. doi:10.1002/2014gc005509
- Worzewski T, Jegen M, Kopp H, Brasse H, Taylor Castillo W (2011) Magnetotelluric image of the fluid cycle in the Costa Rican subduction zone. *Nat Geosci* 4:108–111

**Submit your manuscript to a SpringerOpen<sup>®</sup> journal and benefit from:**

- Convenient online submission
- Rigorous peer review
- Immediate publication on acceptance
- Open access: articles freely available online
- High visibility within the field
- Retaining the copyright to your article

---

Submit your next manuscript at ► [springeropen.com](http://springeropen.com)

---